Hindawi
Journal of Nanomaterials
Volume 2019, Article ID 3281802, 7 pages
https://doi.org/10.1155/2019/3281802

Research Article

Enhanced Antibacterial Activity of Ag Nanoparticle-Decorated ZnO Nanorod Arrays

Jian Shang[1], **Ye Sun**[2], **Teng Zhang**[1], **Zhen Liu**[1] and **Hong Zhang**[2]

[1]*Department of Orthopedics, First Affiliated Hospital of Harbin Medical University, Harbin 150001, China*
[2]*Condensed Matter Science and Technology Institute, School of Science, Harbin Institute of Technology, Harbin 150080, China*

Correspondence should be addressed to Ye Sun; sunye@hit.edu.cn and Teng Zhang; 1142099451@qq.com

Received 15 October 2018; Revised 9 January 2019; Accepted 11 February 2019; Published 30 April 2019

Academic Editor: Angelo Taglietti

Copyright © 2019 Jian Shang et al. This is an open access article distributed under the Creative Commons Attribution License, which permits unrestricted use, distribution, and reproduction in any medium, provided the original work is properly cited.

Silver (Ag) has broad-spectrum antibacterial properties and is widely used in various fields, including in antibacterial coatings for orthopedic implants. For reasons of cost and cytotoxicity, improvement of the antibacterial efficiency of Ag is necessary. The scientific community has also shown a strong enthusiasm in this research area. In this paper, ZnO nanorod arrays were prepared on a titanium (Ti) substrate by seed-assisted hydrothermal method and Ag nanoparticles were deposited by magnetron sputtering to obtain Ag nanoparticle-decorated ZnO nanorod arrays (ZnO nanorods/Ag nanoparticles). The antibacterial properties of ZnO nanorods/Ag nanoparticles against Pseudomonas aeruginosa were systematically studied by agar diffusion method and were compared with other samples such as ZnO nanorod arrays and ZnO seed layer/Ag nanoparticles. The experimental results showed that ZnO nanorods/Ag nanoparticles displayed significantly higher antibacterial properties against Pseudomonas aeruginosa than other samples, including ZnO nanorod arrays and ZnO seed layer/Ag nanoparticles. These superior antibacterial properties originated predominantly from the morphological structure of ZnO nanorods, which optimized the particle size and distribution of Ag nanoparticles, greatly improving their antimicrobial efficiency. The synergistic antibacterial properties of Ag nanoparticles and ZnO nanorods make Ag nanoparticle-decorated ZnO nanorod arrays a promising candidate for antibacterial coating of orthopedic implants.

1. Introduction

In orthopedics, implant-related postoperative infection is a serious complication with a high incidence rate of 1%-4% [1]. In recent years, the excessive use of antibiotics has led to a large number of drug-resistant strains, increasing the postoperative infection rate annually. To curb this and reduce antibiotics abuse, the research on antibacterial coating materials for orthopedic implants has received much attention in the scientific community.

Silver (Ag) nanoparticles have broad-spectrum antibacterial activities and good inhibitory effects on Gram-positive and Gram-negative bacteria, fungi, virus, and cancer cells [2–6], making them one of the most important antimicrobial materials. While increasing the amount of Ag nanoparticle used is the most straightforward method of enhancing the antibacterial properties of Ag-based antibacterial coatings, this method falls short in many aspects. First, the cost of Ag is relatively high. Second, Ag nanoparticles tend to agglomerate when they are present in large numbers, which reduces antibacterial efficacy [7]. The homogeneous distribution of Ag nanoparticles can produce small size and high surface-to-volume ratio of Ag nanoparticles, which can improve the antibacterial effect. In particular, higher Ag dosage may have toxic or side effects on human cells and tissues. For example, overdose of Ag nanoparticles has been reported to suppress the human immune system [8] and induce the production of cytotoxins that damage fibrous tissues in the human lungs [9]. In this sense, improving the antibacterial efficiency of Ag nanoparticles has become a focus of antibacterial coating research. In contrast, zinc oxide (ZnO) has good biocompatibility [10] and low cytotoxicity [11] and promotes the secretion of collagen by osteoblasts and the mineralization of the extracellular matrix [12]. In recent years, ZnO nanomaterials have been found to have good antibacterial activities [13–15] and have attracted much attention as antibacterial materials

because of their low cost, simple preparation, high biocompatibility, and abundant morphological possibilities that are well controllable. A number of Ag/ZnO materials with good antibacterial properties have been prepared by combining the two [16–21]. Recent reported studies focus on the preparation of different types of Ag/ZnO samples, such as Ag/ZnO nanocomposite [18], Ag-containing ZnO films [20], and Ag-doped ZnO nanoparticles [21]. Most of the work is to enhance the antibacterial activity by changing the content or concentration of Ag [20, 21]. Although Ag/ZnO has been reported to improve the antibacterial activity, little in-depth study has been conducted on how to optimize the antibacterial efficiency of Ag by using the synergistic antibacterial effect of Ag and ZnO.

In this study, ZnO nanorod arrays were fabricated on Ti wafer by a modified seed-assisted hydrothermal method [22] and Ag nanoparticles were deposited by magnetron sputtering to develop Ag nanoparticle-decorated ZnO nanorod arrays [23]. The morphology and composition of the samples were characterized by SEM, XRD, and other techniques. The antibacterial properties of ZnO nanorods/Ag nanoparticles and other samples such as ZnO nanorod arrays and ZnO seed layer/Ag nanoparticles against Pseudomonas aeruginosa were studied by agar diffusion. The results of this study confirm the excellent antibacterial properties of ZnO nanorods/Ag nanoparticles and reveal the mechanism of their synergic antibacterial activities.

2. Materials and Methods

2.1. Sample Preparation

2.1.1. Preparation of the ZnO Seed Layer. The ZnO seed layer was fabricated on 10 mm × 10 mm titanium (Ti) wafer by sputtering the ZnO target. The deposition of the seed layer was conducted under the following conditions: temperature of 400°C, oxygen flow rate of 10 sccm, argon flow rate of 40 sccm, working pressure of 1 Pa, and deposition time of 45 s.

2.1.2. Preparation of ZnO Nanorods. Two types of ZnO nanorods were hydrothermally prepared on the ZnO seed layer with zinc nitrate ($Zn(NO_3)_2$)·($6H_2O$, 99%, Sinopharm) and hexamethylenetetramine (HMT) ($C_6H_{12}N_4$, 99%, Aladdin) as precursors. The first type of nanorods was synthesized by warming 50 mL each of 0.1 M $Zn(NO_3)_2$ and HMT at 90°C for 0.5 h and mixing the two solutions in a 130 mL glass bottle. The Ti/seed layer sample was immersed in this mixture, and the glass bottle was sealed. After reacting for 3 h at 90°C, the sample was washed with deionized water and anhydrous ethanol. This Ti/ZnO nanorod sample was named "SG," in which the amount of ZnO was approximately 500 $\mu g/cm^2$. The second type of nanorod was prepared in the same manner, except for using 0.2 M $Zn(NO_3)_2$ and HMT solution.

2.1.3. Preparation of Ag Nanoparticle-Decorated ZnO Nanorod Arrays. Ag nanoparticles were deposited on the two types of ZnO nanorod arrays by radio frequency (RF) magnetron sputtering at room temperature. An RF power of 70 W was used for deposition. The deposition process took place at an argon flow rate of 40 sccm and working pressure of 1 Pa for 30 s. The amount of silver deposited was about 13 $\mu g/cm^2$. The two types of ZnO nanorod/Ag nanoparticle samples obtained were named "SF" and "SE."

2.2. Sample Characterization. The structural properties of the resultant samples were investigated using an X-ray diffractometer (XRD) (PANalytical, X'Pert Pro) with Cu Kα ($\lambda = 0.154$ nm) radiation with a 2θ scanning range of 20°-50°. The surface morphology was examined using scanning electron microscopy (SEM) (FEI Quanta 200F) with an accelerating voltage of 20 kV. An atomic force microscopy (AFM) (Bruker, MultiMode 8) was used for the analysis of the grain diameter.

2.3. Testing the Antibacterial Activity of the Samples. To study in depth the antibacterial properties of ZnO nanorods/Ag nanoparticles, tests were also performed on Ti wafer, hereafter referred to as SA, Ti/Ag nanoparticles (SB), Ti/ZnO seed layer (SC), Ti/ZnO seed layer/Ag nanoparticles (SD), and Ti/ZnO nanorods (SG). The ZnO seed layers and Ag nanoparticles were prepared in the same manner in all samples.

Our antibacterial activity test has been approved by the ISO15189 procedure. The antibacterial effectiveness of the samples was studied by agar diffusion [19, 24, 25]. Pseudomonas aeruginosa (ATCC2785, a Gram-negative bacterium) was used as the prototypical clinical bacteria with blood agar media (Columbia). Pseudomonas aeruginosa was inoculated on blood agar medium and incubated at 37°C for 24 hours. Then some colonies were diluted with 0.9% physiological saline to prepare 10^8 cfu·mL^{-1} suspension. This suspension was inoculated into two identical nutrient agar media N1 and N2. SA, SB, SC, and SD samples were placed into medium N1, and SE, SF, and SG sample were placed into medium N2. The culture media with the respective samples were incubated at 37°C for 48 h in an incubator. The size of the inhibition zone was measured by vernier caliper in millimeters (mm).

3. Results and Discussion

The crystal structure of the samples was first characterized by XRD to prove the successful preparation of ZnO nanorods/Ag nanoparticles. Highly similar XRD spectra were obtained on the ZnO nanorods/Ag nanoparticles samples. As shown in the XRD spectrum of the SF sample in Figure 1, the characteristic peaks of ZnO (100), (002), (101), and (102) are correspond to the wurtzite hexagonal phase of ZnO (JCPDS 03-0888). The diffraction peaks appeared at $2\theta = 38.1°$ corresponding to the cubic-phase Ag (111) (JCPDS 03-0921). Notably, a sharp, strong, and dominant peak of ZnO (002) centered at 34.4° was observed, which was significantly higher than the other ZnO diffraction peaks, revealing the preferential <002> orientation of this sample [26].

In addition, additional flat and broad peaks appeared at $2\theta = 35.5°$ and 40.5°, which have originated from the

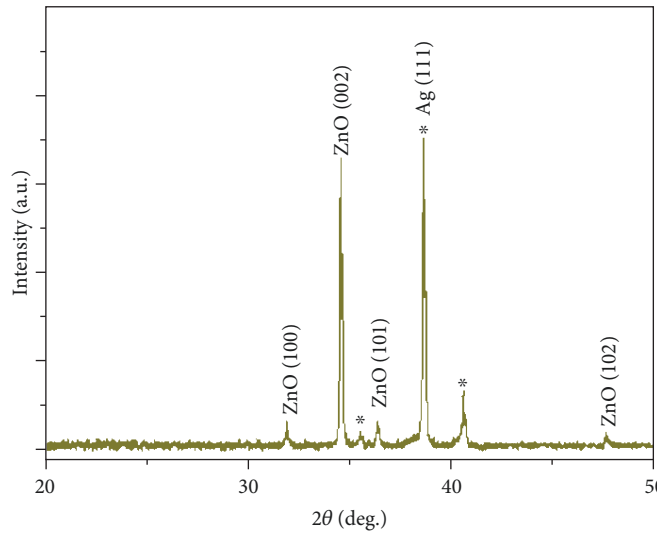

Figure 1: X-ray diffraction spectrum of the ZnO nanorod/Ag nanoparticle (SF) sample. The peaks marked with an asterisk are associated with the titanium alloy plate.

titanium alloy plate substrate. These results indicated the formation of highly crystalline ZnO and Ag in this work.

The SEM images of ZnO nanorod/Ag nanoparticle samples are displayed in Figure 2. Figure 2(a) is the top-view SEM image of SF at low magnification, in which numerous uniformly distributed hexagonal prism-like nanorods can be seen. This is consistent with the typical morphology of ZnO nanorods reported in the literature [27–29]. Most nanorods grow perpendicular to the Ti substrate, forming highly <002> oriented nanorod arrays, as also shown in the XRD data. These nanorods were mostly even in diameter, with an average diameter of about 85 nm. Signs of Ag nanoparticles are not evident in the low-magnification SEM image of Figure 2(a), as the number and size of Ag nanoparticles are much smaller than those of ZnO nanorods. The surface of pure ZnO nanorods was smooth. In the high-magnification top-view SEM image of SF (Figure 2(b)), we can clearly observe the rough surface of nanorods, which corresponds to Ag nanoparticles (AgNPs) with uniform sizes, confirming the successful fabrication of Ag nanoparticle-modified ZnO nanorod arrays. The morphology of SE samples is also characterized by low- and high-magnification SEM images (Figures 2(c) and 2(d), respectively). In Figure 2(c), SE also contains a large number of hexagonal prism nanorods with preferential orientation. They had a diameter of approximately 135 nm, which is significantly greater than the diameter of the nanorods in SF samples, as the ZnO nanorods in SE were prepared from precursors with higher concentrations.

Figure 2(d) shows that the surface of nanorods in SE samples is also covered by nanoparticles. As indicated in these SEM results, the sizes of Ag nanoparticles in both ZnO nanorod/Ag nanoparticle samples were very small, in the range of 10-20 nm. The nanoparticles formed here were significantly smaller than those in the Ti/ZnO seed layer/Ag nanoparticle samples, which were measured by AFM to have sizes of 40-100 nm (Figure 3). These results confirmed the successful preparation of highly crystalline ZnO nanorods/Ag nanoparticles and that ZnO nanorod arrays had a substantial effect on the size and distribution of Ag nanoparticles.

The antimicrobial activity of the samples was determined by the size of the Pseudomonas aeruginosa inhibition zone formed. Figure 4 shows the bacteria inhibition rings produced by SA, SB, SC, SD, SE, SF, and SG samples after 24 h of culturing in an incubator at 37°C. In medium N1, no distinct bacterial inhibition zone is observed around samples SA (Ti wafer), SB (Ti/Ag nanoparticles), and SC (Ti/ZnO seed layer), while a small bacterial inhibition zone is seen around sample SD (Ti/ZnO seed layer/Ag nanoparticles). These results showed that the ZnO seed layer or Ag nanoparticles on the Ti substrate alone had no appreciable antibacterial activity against Pseudomonas aeruginosa but a combination of the two could give synergic antibacterial effect. Sample SB should have antibacterial activity, but we did not see the obvious inhibition zone in our work. It may be due to the agglomeration of Ag nanoparticles, which weakens the antibacterial effect and results in the low concentration of Ag ions released into the surrounding environment.

In the N2 medium, noticeable bacterial inhibition zones were formed around the SE, SF, and SG samples. The inhibition zone formed by SG (ZnO nanorods) was smaller and had a diameter of 11.5 mm, while those by SE and SF (two ZnO nanorod/Ag nanoparticle samples) were larger and had diameters of 13.1 mm and 13.2 mm, respectively. The antibacterial properties of ZnO and Ag were then studied in depth by comparing the antibacterial actions of different samples. First, the antibacterial properties of SG (ZnO nanorods) were similar to those of SD (ZnO seed layer/Ag nanoparticles). The amount of ZnO in the SG sample was about 500 μg/cm^2, while the amount of Ag deposited in the SD sample was about 13 μg/cm^2. Therefore, ZnO nanorods, although had some antibacterial effects on Pseudomonas

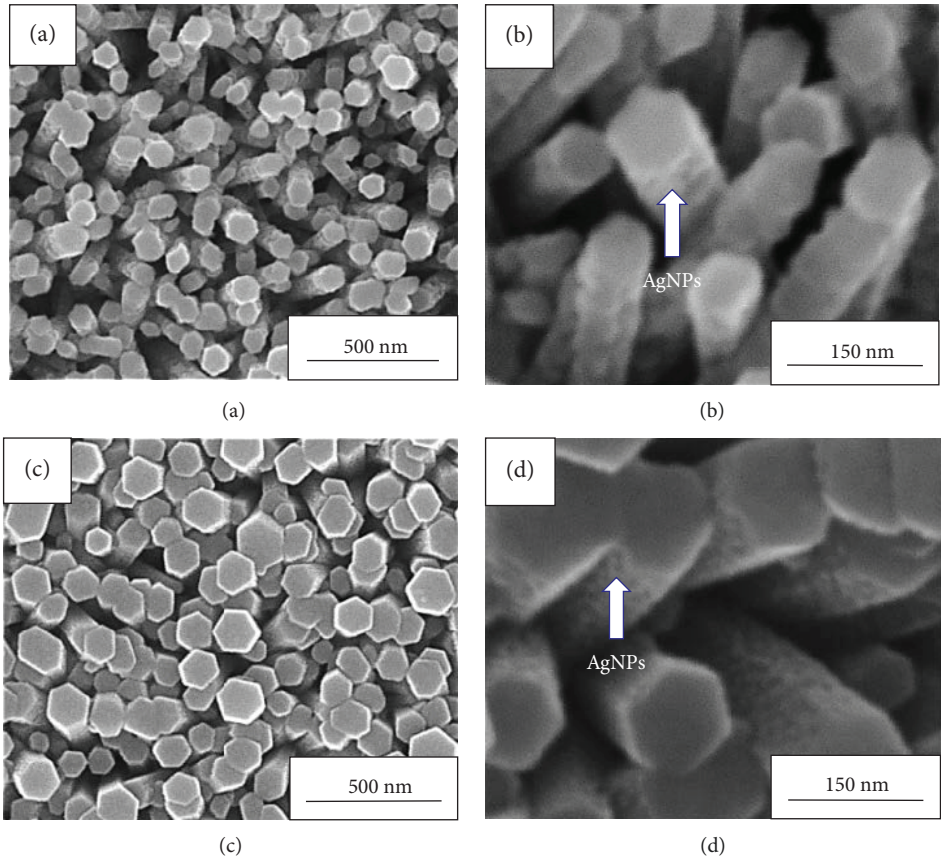

Figure 2: Scanning electron microscopy images of the SF (a, b) and SE (c, d) samples.

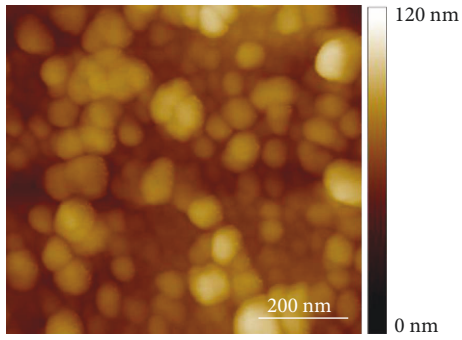

Figure 3: Atomic force microscopy image of the SD sample.

aeruginosa, were much less capable of doing so than Ag nanoparticles [30]. When the antibacterial functions of SF (ZnO nanorods/Ag nanoparticles) and SD (ZnO seed layer/Ag nanoparticles) were compared, the far more superior antibacterial activities of the former were clearly not only caused by the difference between ZnO nanorods and the ZnO seed layer in this respect. Hence, the Ag nanoparticles on ZnO nanorods had higher antibacterial capability than those on the ZnO seed layer, although the same total amount of Ag was present in both cases. As shown in Figure 2(b), the particle size of Ag nanoparticles in the SF sample ranges from 10 to 20 nm, much less than the 40-100 nm size of Ag nanoparticles on the seed layer (Figure 3). This could be the reason for the higher antibacterial activities of Ag nanoparticles on ZnO nanorods, i.e., the morphology and large surface area of the nanorods make it possible for Ag nanoparticles to distribute over a greater area on the nanorods and have a larger surface area, facilitating the antimicrobial action of the latter [31]. In addition, the key mechanism for Ag nanoparticles to exert antibacterial activity is through the release of Ag ions. As the size of nanoparticles decreases, the surface area will increase. The release rate of Ag ions is proportional to the surface area of the particles, so the release rate of Ag ions from smaller nanoparticles is faster than that of larger nanoparticles, which improves the antibacterial properties of Ag nanoparticles [32, 33]. On the contrary, although SE samples definitely contain more ZnO than SF samples, the antibacterial activities of the two come very close, with SE being even lower by a small amount. This is another proof of Ag nanoparticles as the primary origin of antibacterial functions in ZnO nanorods/Ag nanoparticles, despite some antibacterial properties being detected in ZnO nanorods. In contrast, SB (Ti/Ag nanoparticles) samples showed almost no antibacterial effect. The above evidence leads to the conclusion that the synergic antibacterial activities of ZnO nanorods and Ag nanoparticles were mainly derived from the morphology and structure of ZnO nanorods, which optimized the size and distribution of Ag nanoparticles and greatly improved their antibacterial efficiency.

Figure 5 shows the changes in the inhibition zones of SD, SE, SF, and SG cultured for different durations in an incubator at 37°C. Strong antibacterial activities are seen in all four

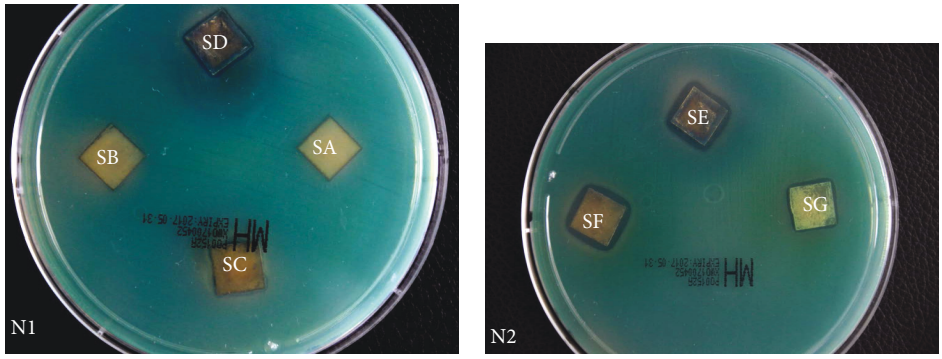

(a) (b)

Figure 4: The size of the inhibition zone of Pseudomonas aeruginosa after 24 h of culture.

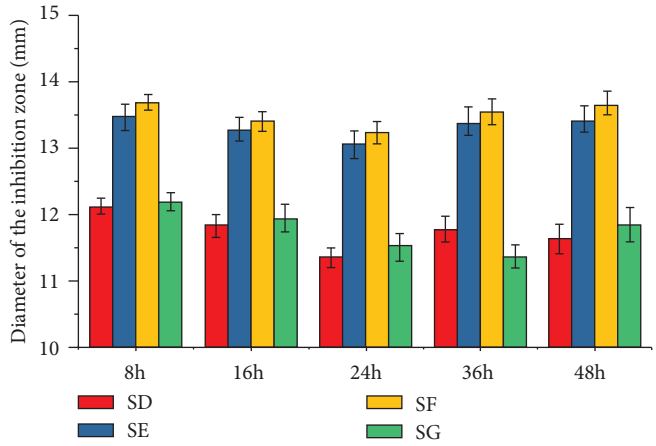

Figure 5: The inhibition zone test of the SD, SE, SF, and SG samples at different times.

samples within 48 h. The diameters of the inhibition zones at 48 h were similar to those at 8 h, which may be related to the diffusion of Ag ions in the agar media, and the antibacterial activity mainly depended on the active surface area of Ag in the agar media [34]. The bacterial inhibition zones of SD and SG had similar diameters, as well as those of SF and SE samples. The diameters of the inhibition zones of SE samples at 8, 16, 24, 36, and 48 hours were 13.5, 13.3, 13.1, 13.4, and 13.5 mm, respectively. Similarly, the inhibition zones of SF samples were 13.7, 13.4, 13.2, 13.5, and 13.7 mm, respectively. With prolonged incubation, the diameters of the inhibition zones formed by SF and SE were maintained at 13.1-13.7 mm, proving the superior long-term antibacterial properties of ZnO nanorods/Ag nanoparticles.

4. Conclusions

In summary, ZnO nanorods/Ag nanoparticles were prepared on a Ti substrate using both gas- and liquid-phase methods. Their excellent synergic antibacterial properties were confirmed with Pseudomonas aeruginosa as the target. Comparison with other samples was also carried out as verification. Although ZnO nanorods alone also have some antibacterial effects, the superiority of ZnO nanorods/Ag nanoparticles in this respect was mainly derived from the morphological structure of ZnO nanorods, which optimized the size and distribution of Ag nanoparticles and greatly enhanced their antibacterial efficacy. Improving the antibacterial efficiency of Ag nanoparticles reduces the cytotoxicity induced by high dosage of Ag and lowers the cost of antibacterial coating. Because of its synergic antibacterial activity, this type of ZnO nanorod/Ag nanoparticle material will have broad usage prospects as antibacterial coatings on orthopedic implants. In addition, this work provides a novel route for the synthesis of Ag-based coatings with higher antibacterial efficiency.

Data Availability

The data used to support the findings of this study are included within the article.

Conflicts of Interest

The authors declare that they have no conflicts of interest.

Acknowledgments

This work was financially supported by the Science and Technology Research Project of Heilongjiang Provincial Education Department (12541344).

References

[1] B. Laure, J. M. Besnier, A. M. Bergemer-Fouquet et al., "Effect of hydroxyapatite coating and polymethyimemacrylate on stainless steel implant site infection with *Staphylococcus epidermids* in a sleep model," *Journal of Biomedical Materials Research Part A*, vol. 84A, no. 1, pp. 92–98, 2008.

[2] I. Sondi and B. Salopek-Sondi, "Silver nanoparticles as antimicrobial agent: a case study on *E.coli* as a model for Gram-negative bacteria," *Journal of Colloid and Interface Science*, vol. 275, no. 1, pp. 177–182, 2004.

[3] W.-R. Li, X. B. Xie, Q. S. Shi, H. Y. Zeng, Y. S. OU-Yang, and Y. B. Chen, "Antibacterial activity and mechanism of silver nanoparticles on *Escherichia coli*," *Applied Microbiology and Biotechnology*, vol. 85, no. 4, pp. 1115–1122, 2010.

[4] Z. K. Xia, Q. H. Ma, S. Y. Li et al., "The antifungal effect of silver nanoparticles on *Trichosporon asahii*," *Journal of Microbiology, Immunology and Infection*, vol. 49, no. 2, pp. 182–188, 2016.

[5] S. Gaikwad, A. Ingle, A. Gade et al., "Antiviral activity of mycosynthesized silver nanoparticles against herpes simplex virus and human parainfluenza virus type 3," *International Journal of Nanomedicine*, vol. 8, no. 1, pp. 4303–4314, 2013.

[6] M. Jeyaraj, M. Rajesh, R. Arun et al., "An investigation on the cytotoxicity and caspase-mediated apoptotic effect of biologically synthesized silver nanoparticles using *Podophyllum hexandrum* on human cervical carcinoma cells," *Colloids and Surfaces B: Biointerfaces*, vol. 102, no. 1, pp. 708–717, 2013.

[7] F. Ghilini, M. C. Rodríguez González, A. G. Miñán et al., "Highly stabilized nanoparticles on poly-L-lysine-coated oxidized metals: a versatile platform with enhanced antimicrobial activity," *ACS Applied Materials & Interfaces*, vol. 10, no. 28, pp. 23657–23666, 2018.

[8] W. H. de Jong, L. T. M. van der Ven, A. Sleijffers et al., "Systemic and immunotoxicity of silver nanoparticles in an intravenous 28 days repeated dose toxicity study in rats," *Biomaterials*, vol. 34, no. 33, pp. 8333–8343, 2013.

[9] P. V. AshaRani, G. Low Kah Mun, M. P. Hande, and S. Valiyaveettil, "Cytotoxicity and genotoxicity of silver nanoparticles in human cells," *ACS Nano*, vol. 3, no. 2, pp. 279–290, 2009.

[10] K. Huo, X. Zhang, H. Wang, L. Zhao, X. Liu, and P. K. Chu, "Osteogenic activity and anti-bacterial effects on titanium surfaces modified with Zn-incorporated nanotube arrays," *Biomaterials*, vol. 34, no. 13, pp. 3467–3478, 2013.

[11] G. J. Nohynek, E. Antignac, T. Re, and H. Toutain, "Safety assessment of personal care products/cosmetics and their ingredients," *Toxicology and Applied Pharmacology*, vol. 243, no. 2, pp. 239–259, 2010.

[12] G. Jin, H. Cao, Y. Qiao, F. Meng, H. Zhu, and X. Liu, "Osteogenic activity and antibacterial effect of zinc ion implanted titanium," *Colloids and Surfaces B: Biointerfaces*, vol. 117, no. 9, pp. 158–165, 2014.

[13] G. Applerot, N. Perkas, G. Amirian, O. Girshevitz, and A. Gedanken, "Coating of glass with ZnO via ultrasonic irradiation and a study of its antibacterial properties," *Applied Surface Science*, vol. 256, no. 3, pp. S3–S8, 2009.

[14] K. H. Tam, A. B. Djurišić, C. M. N. Chan et al., "Antibacterial activity of ZnO nanorods prepared by a hydrothermal method," *Thin Solid Films*, vol. 516, no. 18, pp. 6167–6174, 2008.

[15] M. Ramani, S. Ponnusamy, and C. Muthamizhchelvan, "Preliminary investigations on the antibacterial activity of zinc oxide nanostructures," *Journal of Nanoparticle Research*, vol. 15, no. 4, p. 1557, 2013.

[16] S. Ghosh, V. S. Goudar, K. G. Padmalekha, S. V. Bhat, S. S. Indi, and H. N. Vasan, "ZnO/Ag nanohybrid: synthesis, characterization, synergistic antibacterial activity and its mechanism," *RSC Advances*, vol. 2, no. 3, pp. 930–940, 2012.

[17] D. V. Ponnuvelu, S. P. Suriyaraj, T. Vijayaraghavan, R. Selvakumar, and B. Pullithadathail, "Enhanced cell-wall damage mediated, antibacterial activity of core–shell ZnO@Ag heterojunction nanorods against *Staphylococcus aureus* and *Pseudomonas aeruginosa*," *Journal of Materials Science: Materials in Medicine*, vol. 26, no. 7, p. 204, 2015.

[18] S. Wang, J. Wu, H. Yang, X. Liu, Q. Huang, and Z. Lu, "Antibacterial activity and mechanism of Ag/ZnO nanocomposite against anaerobic oral pathogen *Streptococcus mutans*," *Journal of Materials Science: Materials in Medicine*, vol. 28, no. 1, p. 23, 2017.

[19] A. H. Shah, E. Manikandan, M. Basheer Ahmed, and V. Ganesan, "Enhanced bioactivity of Ag/ZnO nanorods-a comparative antibacterial study (Sbds)," *Journal of Nanomedicine & Nanotechnology*, vol. 4, no. 3, p. 1, 2013.

[20] T. Fu, F. Zhang, Z. Alajmi, S. Y. Yang, F. Wu, and S. L. Han, "Sol-gel derived antibacterial Ag-containing ZnO films on biomedical titanium," *Journal of Nanoscience and Nanotechnology*, vol. 18, no. 2, pp. 823–828, 2018.

[21] G. Y. Nigussie, G. M. Tesfamariam, B. M. Tegegne et al., "Antibacterial activity of Ag-doped TiO_2 and Ag-doped ZnO nanoparticles," *International Journal of Photoenergy*, vol. 2018, Article ID 5927485, 7 pages, 2018.

[22] Y. Yin, Y. Sun, M. Yu et al., "Controlling the hydrothermal growth and the properties of ZnO nanorod arrays by pretreating the seed layer," *RSC Advances*, vol. 4, no. 84, pp. 44452–44456, 2014.

[23] A. S. M. Iftekhar Uddin and G. S. Chung, "A novel flexible C_2H_2 gas sensor based on Ag-ZnO nanorods on PI/PTFE substrate," in *Proceedings Volume 9749, Oxide-based Materials and Devices VII; 97491T*, San Francisco, CA, USA, February 2016.

[24] L. Lei, X. Liu, Y. Yin, Y. Sun, M. Yu, and J. Shang, "Antibacterial Ag–SiO_2 composite films synthesized by pulsed laser deposition," *Materials Letters*, vol. 130, pp. 79–82, 2014.

[25] S. C. Motshekga, S. S. Ray, M. S. Onyango, and M. N. B. Momba, "Microwave-assisted synthesis, characterization and antibacterial activity of Ag/ZnO nanoparticles supported bentonite clay," *Journal of Hazardous Materials*, vol. 262, no. 262, pp. 439–446, 2013.

[26] Y. Yin, Y. Sun, M. Yu et al., "Arrays of nanorods composed of ZnO nanodots exhibiting enhanced UV emission and stability," *Nanoscale*, vol. 6, no. 18, pp. 10746–10751, 2014.

[27] Y. Yin, Y. Sun, M. Yu et al., "Reagent concentration dependent variations in the stability and photoluminescence of silica-coated ZnO nanorods," *Inorganic Chemistry Frontiers*, vol. 2, no. 1, pp. 28–34, 2015.

[28] Y. Yin, Y. Sun, M. Yu et al., "ZnO nanorod array grown on Ag layer: a highly efficient fluorescence enhancement platform," *Scientific Reports*, vol. 5, no. 1, article 8152, 2015.

[29] Y. Sun, N. A. Fox, D. J. Riley, and M. N. R. Ashfold, "Hydrothermal growth of ZnO nanorods aligned parallel to the

substrate surface," *Journal of Physical Chemistry C*, vol. 112, no. 25, pp. 9234–9239, 2008.

[30] J. F. Hernández-Sierra, F. Ruiz, D. C. Cruz Pena et al., "The antimicrobial sensitivity of *Streptococcus mutans* to nanoparticles of silver, zinc oxide, and gold," *Nanomedicine: Nanotechnology, Biology, and Medicine*, vol. 4, no. 3, pp. 237–240, 2008.

[31] Y. Chen, W. H. Tse, L. Chen, and J. Zhang, "Ag nanoparticles-decorated ZnO nanorod array on a mechanical flexible substrate with enhanced optical and antimicrobial properties," *Nanoscale Research Letters*, vol. 10, no. 1, p. 106, 2015.

[32] C. Marambio-Jones and E. M. V. Hoek, "A review of the antibacterial effects of silver nanomaterials and potential implications for human health and the environment," *Journal of Nanoparticle Research*, vol. 12, no. 5, pp. 1531–1551, 2010.

[33] M. Rai, A. Yadav, and A. Gade, "Silver nanoparticles as a new generation of antimicrobials," *Biotechnology Advances*, vol. 27, no. 1, pp. 76–83, 2009.

[34] M. Boswald, M. Girisch, J. Greil et al., "Antimicrobial activity and biocompatibility of polyurethane and silicone catheters containing low concentrations of silver: a new perspective in prevention of polymer-associated foreign-body-infections," *Zentralblatt für Bakteriologie*, vol. 283, no. 2, pp. 187–200, 1995.


The Scientific
World Journal
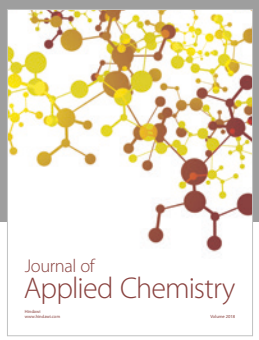
Journal of
Applied Chemistry
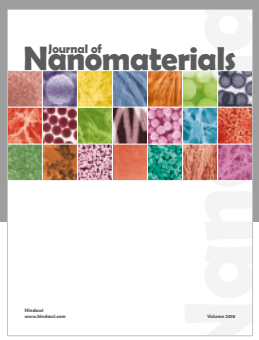
Journal of
Nanomaterials

Scientifica

International Journal of
Polymer Science
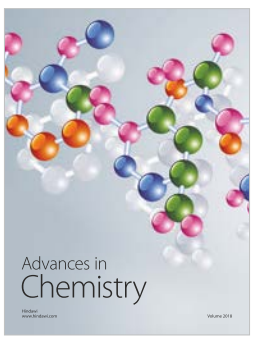
Advances in
Chemistry

Hindawi
Submit your manuscripts at
www.hindawi.com
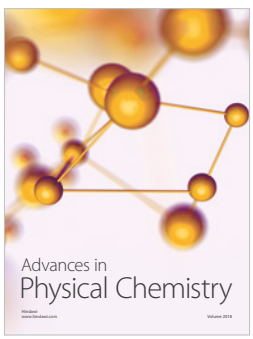
Advances in
Physical Chemistry

International Journal of
Analytical Chemistry
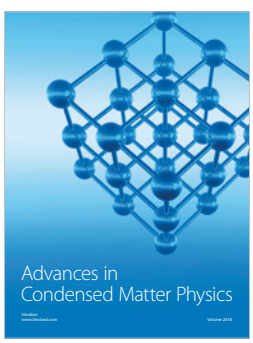
Advances in
Condensed Matter Physics
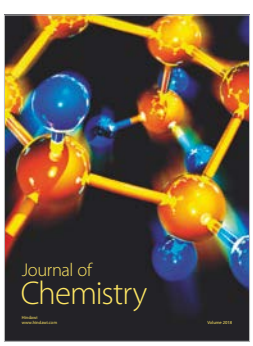
Journal of
Chemistry

International Journal of
Biomaterials
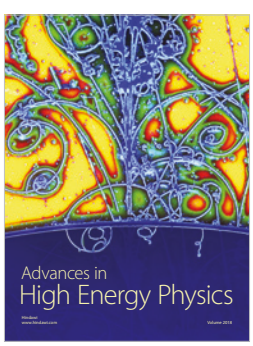
Advances in
High Energy Physics

Journal of
Engineering

Journal of
Nanotechnology

International Journal of
Corrosion

Journal of
Materials

BioMed
Research International
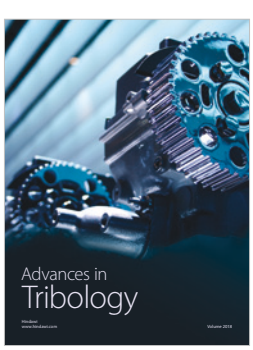
Advances in
Tribology
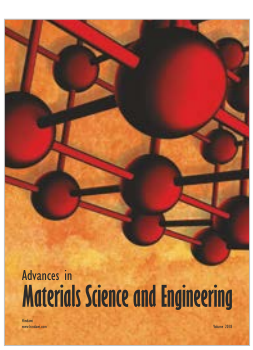
Advances in
Materials Science and Engineering